BBA - Molecular Basis of Disease 1870 (2024) 167187

Contents lists available at ScienceDirect

BBA - Molecular Basis of Disease

journal homepage: www.elsevier.com/locate/bbadis

miR-519a-3p, found to regulate cellular prion protein during Alzheimer's disease pathogenesis, as a biomarker of asymptomatic stages

Dayaneth Jácome [a,b], Tiziana Cotrufo [a,b,c], Pol Andrés-Benito [d,e], Laia Lidón [a,b,c,d,1], Eulàlia Martí [c,f,g], Isidre Ferrer [c,d,h,i], José Antonio del Río [a,b,c,d,2], Rosalina Gavín [a,b,c,d,2,*]

[a] Molecular and Cellular Neurobiotechnology, Institute for Bioengineering of Catalonia, Barcelona, Spain
[b] Department of Cell Biology, Physiology and Immunology, University of Barcelona, Barcelona, Spain
[c] Institute of Neuroscience, University of Barcelona, Barcelona, Spain
[d] Center for Networked Biomedical Research in Neurodegenerative Diseases (CIBERNED), Barcelona, Madrid, Spain
[e] Neurologic Diseases and Neurogenetics Group, Bellvitge Institute for Biomedical Research (IDIBELL), L'Hospitalet de Llobregat, Barcelona, Spain
[f] Functional Genomics of Neurodegenerative Diseases, Department of Biomedical Sciences, University of Barcelona, Barcelona, Spain
[g] CIBERESP (Centro en Red de Epidemiología y Salud Pública), Spain
[h] Department of Pathology and Experimental Therapeutics, University of Barcelona, Barcelona, Spain
[i] Senior Consultant Neuropathology, Service of Pathology, Bellvitge University Hospital, Hospitalet de Llobregat, Spain

ARTICLE INFO

Keywords:
Cellular prion protein
Alzheimer's disease
MicroRNAs
Biomarker

ABSTRACT

Clinical relevance of miRNAs as biomarkers is growing due to their stability and detection in biofluids. In this, diagnosis at asymptomatic stages of Alzheimer's disease (AD) remains a challenge since it can only be made at autopsy according to Braak NFT staging. Achieving the objective of detecting AD at early stages would allow possible therapies to be addressed before the onset of cognitive impairment. Many studies have determined that the expression pattern of some miRNAs is dysregulated in AD patients, but to date, none has been correlated with downregulated expression of cellular prion protein (PrP^C) during disease progression. That is why, by means of cross studies of miRNAs up-regulated in AD with *in silico* identification of potential miRNAs-binding to 3′UTR of human *PRNP* gene, we selected miR-519a-3p for our study. Then, *in vitro* experiments were carried out in two ways. First, we validated miR-519a-3p target on 3′UTR-*PRNP*, and second, we analyzed the levels of PrP^C expression after using of mimic technology on cell culture. In addition, RT-qPCR was performed to analyzed miR-519a-3p expression in human cerebral samples of AD at different stages of disease evolution. Additionally, samples of other neurodegenerative diseases such as other non-AD tauopathies and several synucleinopathies were included in the study.

Our results showed that miR-519a-3p overlaps with *PRNP* 3′UTR *in vitro* and promotes downregulation of PrP^C. Moreover, miR-519a-3p was found to be up-regulated exclusively in AD samples from stage I to VI, suggesting its potential use as a novel label of preclinical stages of the disease.

Abbreviations: Aβ, β-amyloid; AD, Alzheimer's disease; CBD, corticobasal degeneration; CNS, central nervous system; CSF, cerebrospinal fluid; GGT, glial globular tauopathy; MCI, mild cognitive impairment; MMSE, Mini-Mental Scale examination; NDD, neurodegenerative disease; NFT, neurofilament tangles; nND, non-neurodegenerative controls; PD, Parkinson's disease; PDD, PD-associated dementia; PET, positron emission tomography; PHF, paired helical filaments; PiD, Pick's disease (PiD); PrP^C, cellular prion protein.

* Corresponding author at: Department of Cell Biology, Physiology and Immunology, University of Barcelona, Barcelona, Spain.
E-mail addresses: djacome@ibecbarcelona.eu (D. Jácome), tcotrufo@ibecbarcelona.eu (T. Cotrufo), pol.andres.benito@gmail.com (P. Andrés-Benito), llidon@santpau.cat (L. Lidón), eulalia.marti@ub.edu (E. Martí), 8082ifa@gmail.com (I. Ferrer), jadelrio@ibecbarcelona.eu (J.A. del Río), rgavin@ub.edu (R. Gavín).
[1] Current address: Memory Unit, Neurology Department, Hospital de Sant Pau, Barcelona, Spain.
[2] Senior co-authors.

https://doi.org/10.1016/j.bbadis.2024.167187
Received 14 December 2023; Received in revised form 11 April 2024; Accepted 16 April 2024
Available online 21 April 2024

1. Introduction

1.1. Alzheimer's disease and its current diagnosis status

Alzheimer's disease (AD), despite being the most common cause of dementia, is far from having an early diagnosis, before mild or moderate cognitive deterioration appears and despite being the most common cause of dementia. This makes early therapeutic intervention, which is currently restricted to 4 FDA-approved drugs unable to significantly reduce cognitive decline or improve global functioning, very difficult to realize.

As widely described, one of the neuropathological hallmarks of AD is extracellular accumulation of senile plaques, enriched in β-amyloid (Aβ) peptide. In addition, AD pathology develops like other tauopathies with intracellular aggregates of hyperphosphorylated tau protein into paired helical filaments (PHF), and then into neurofilament tangles (NFT). These are deposited progressively, starting in the entorhinal cortex and hippocampus and then spreading across other brain regions [1–4]. In this sense, classical longitudinal studies of cognitive function and cerebrospinal fluid (CSF) analysis, as well as the switch from neuroimaging biomarkers used in dementia to AD-specific markers, have identified a significant preclinical phase of the disease that precedes onset of symptoms by anywhere from 10 to 20 years. This is characterized by early Aβ deposition in the precuneus and other cortical regions, followed sequentially by regional cortical hypometabolism, significant accumulation of tau pathology, and the onset of symptomatic cognitive impairment. Unlike Aβ, and as previously reported, the stage of tau pathology correlates well with the progression of cognitive decline [5], largely following the Braak stages (I to VI) according to the regional distribution of NFT after *post-mortem* evaluation [6].

In general terms, neuropathological diagnosis of AD can currently be made with reasonable certainty using CSF or positron emission tomography (PET) imaging biomarkers that allow estimation of cerebral Aβ and tau depositions [7,8]. However, in some cases, cognitive impairment and behavioural changes are not apparent until severe AD dementia, preventing a reliable diagnosis. In addition, with the use of cognitive scales such as the Mini-Mental Scale examination (MMSE), people in Braak stage I-II are seen to be asymptomatic and considered healthy, as shown by correlating the scores of the Braak staging and MMSE results [9]. Moreover, in clinical practice, there are no standardized criteria for diagnosis, and there may be serious variations between centres including heterogeneous methodologies as well as expensive and/or invasive ones [10–12]. In this line, the use of CSF carries the risks and inconveniences involved in a lumbar puncture procedure. Current trends are focused on the search for markers (some of them in the line of epigenetics; see below) in tissue extracted using non-invasive procedures [13,14]. The detection of peripheral biomarkers in samples such as blood is emerging as an advance in terms of the correlation of classical biomarkers in CSF and PET images [15,16] (collected at [17]). However, general population screening continues to be a long-term goal [18].

Among epigenetic signatures in AD, a large number of studies show the dysregulation of various microRNAs (miRNAs) in the disease. Importantly, the potential of miRNAs as diagnostic tools has been widely reported, as they show a regular pattern among various body fluids [19,20] and a marked correlation between the expression levels in plasma and brain parenchyma [21]. In this regard, miR-519a-3p has already been proposed as a biomarker of AD in patients showing mild cognitive impairment (MCI) [22–25] and it has been found in various fluids such as CSF, blood, plasma, and serum. However, its potential as a biomarker of asymptomatic stages (according to Braak stages I and II) has never been analyzed before.

Epigenetic signature of cellular prion protein as possible blood biomarker for AD.

The relationship between cellular prion protein (PrP^C) and AD is widely reported. PrP^C was initially known to be the causative agent of prionopathies when it undergoes changes in its normal folding [26]. However, its physiological role is still a subject of debate, and some studies show its interaction/participation with proteins or signalling pathways involved in AD (see some examples in [27–29]). Even so, the role of PrP^C in the disease remains unresolved, since some studies grant it a pathogenic role [30] while others support a neuroprotective function (*e.g.* [31] reviewed in [32]).

PrP^C is mainly expressed by neurons and glial cells in the adult central nervous system (CNS) [33–35], and in humans it is encoded in a single gene, *PRNP*, whose sequence is highly conserved in vertebrates [36]. Relevantly, the PrP^C expression profile varies during development [35,37,38] with ageing in adults [39] and during AD progression; it shows higher levels of expression in asymptomatic stages of the disease [40–42] and a progressive reduction in advanced stages.

To date there is no known mechanism involved in the reduction of PrP^C levels in the progression of AD, although abundant miRNA binding sites in the *PRNP* 3′UTR are known to be responsible for reduction [43]. The aforementioned study showed the binding of some miR-519 family members (b-3p and d-3p) to the *PRNP* 3′UTR.

Therefore, in the present study, we first cross-checked data from miRWalk, miRanda, RNA22, and Targetscan databases to select putative miRNAs responsible for the reduction of PrP^C during AD progression, pointing up miR-519a-3p as a candidate. Then, we demonstrated *in vitro* functional reduction of PrP^C by miR-519a-3p using mimic technology. Next, we analyzed miR-519a-3p expression in frontal cortex samples of AD (from Braak I to VI) and other neurodegenerative disease (NDD) such as non-AD tauopathies and synucleopathies. In this way, we revealed early and exclusive expression of the miR-519a-3p in AD as a useful tool to generate a novel AD-specific signature in asymptomatic stages of the disease.

2. Materials and methods

2.1. miR-519a-3p selection for the study

In silico prediction of potential miRNAs with *PRNP* 3′UTR as target was made crossing data from the miRWalk, miRanda, RNA22, and Targetscan databases. After that, candidates were analyzed for reported overexpression in AD [44]. Finally, miR-519a-3p (AAAGUGCAUCCUUUUAGAGUGU) was selected as the main candidate, taking into account that it has already been found in various fluids such as CSF, blood, plasma, and serum in patients with mild cognitive impairment (MCI) and AD [22–25].

2.2. Cell culture and transfection

CCF-STTG1 human grade IV astrocytoma cells (CRL-1718, American Type Culture Collection (ATCC)) were used to analyse the levels of PrP^C *in vitro* after has-miR-519a-3p Mimic (Qiagen) transfection. Cells were maintained in Roswell Park Memorial Institute (RPMI) 1640 medium supplemented with 10 % fetal bovine serum (FBS), and 1 % penicillin/streptomycin (Thermo Fisher Scientific, MA, USA), in 75 cm^2 culture bottles (Nunc, Denmark) maintained in a 5 % CO_2 atmosphere at 37 °C. One week before transfection, cells were cultured in the same medium, on poly-D-lysine (Sigma-Aldrich, Darmstadt, Germany) coated 6-well plates (Nunc, Denmark).

HEK293 human embryonic kidney cells (ATCC CRL-1573, American Type Culture Collection, Rockville, Md., USA) were used to perform *in vitro* miR-519a-3p target analysis on 3′UTR-*PRNP* reporter construct (vector pEZX-MT06, Genecopoeia). Cells were maintained in Advanced Dulbecco's modified Eagle's medium (AdDMEM) supplemented with 10 % fetal bovine serum (FBS), 0.5 % glutamine, and 1 % penicillin/streptomycin (Thermo Fisher Scientific, MA, USA) in 75 cm^2 culture bottles (Nunc, Denmark) in a 5 % CO_2 atmosphere at 37 °C. One day before cotransfection, cells were cultured in the same medium, on poly-D-lysine-coated (Sigma-Aldrich, Darmstadt, Germany) 24-well plates

(Nunc, Denmark).

Transfections were performed using Lipofectamine 2000 (Invitrogen-Thermo Fisher Scientific) according to the manufacturer's instructions.

2.3. Human samples

The brains of non-neurodegenerative controls (nND) and patients with AD, other non-AD tauopathies, and synucleinopathies were obtained after death and were immediately prepared for morphological and biochemical study.

A total of 25 hippocampal postmortem samples were obtained from HUB-ICO-IDIBELL Biobank to be analyzed in this study. The cases comprised nND (n = 6) and AD (n = 19). See Supplementary Table 1 for additional data. In addition, a total of 106 frontal cortex (area 8) postmortem samples were obtained from Clinic-IDIBAPS, HUB-ICO-IDIBELL, and NAVARRABIOMED Biobanks following the guidelines of Spanish legislation on this matter and approval of the local ethics committees. Total cases comprised nND (n = 14), AD (n = 61), non-AD tauopathies (n = 10), and synucleinopathies (n = 21).

Following neuropathological examination, AD cases were categorized according to neurofibrillary tangles (stages I to VI) and Aβ deposition (stages A, B and C) [6,45]. Non-AD tauopathies included corticobasal degeneration (CBD), (n = 4), glial globular tauopathy (GGT), (n = 3), and Pick's disease (PiD) (n = 3). Synucleinopathies comprised Parkinson's disease (PD, n = 21), 3 of them with associated dementia (PDD, n = 3). Neuropathological staging of these cases was based on the classification of Braak, from 1 to 6 [46]. Finally, nND cases did not show neurological or metabolic disease, and the neuropathological examination, carried out in similar regions and with the same methods as in pathological cases of this study, did not show lesions. In particular, no amyloid, tau, or α-synuclein deposits were seen in the regions examined. A summary of basic patient data is presented in Supplementary Table 2.

2.4. RT-qPCR

Total RNA from human hippocampal/frontal cortex samples and cultured cells was extracted with mirVana's isolation kit (Ambion, TX, USA) following the manufacturer's instructions. Total purified RNAs were used to generate the corresponding cDNAs, which served as PCR templates for qPCR assays. Before this, total RNA was quantified by qubit and analyzed for RNA integrity (RIN) by the geomics service of Scientific and Technological services of the UB (CCiTUB). Retrotranscription (RT) was performed using the miRCURY LNA RT kit (Qiagen, Germany).

Quantitative PCR (qPCR) for miR-519a-3p was performed with three technical replicates in triplicate using miRCURY LNA SYBR Green PCR kit (Qiagen) and hsa-miR-519a-3p, LNA™ PCR primer set (Qiagen). PCR amplification and detection were performed with the Applied Biosystems StepOnePlus Real-Time detector. The following thermal profile was applied: 1 cycle at 95 °C for 2 min, 40 cycles at 95 °C for 10 s, and 56 °C for 60 s. Melting curve analysis was performed at 95 °C for 15 s, 60 °C for 60 s, and 95 °C for 15 s. miRNA levels were calculated using the StepOne™ software v2.3, following the $2^{-\Delta\Delta CT}$ method of Applied Biosystems [47]. Samples were normalized for the relative expression of the housekeeping gen miR103a-3p (hsa-miR-103a-3p, LNA™ PCR primer set, Qiagen), which showed no variability between analyzed groups (Supplementary Fig. 1).

RT-qPCR for *PRNP* mRNA was performed with three technical replicates using the following primers: (5′-agtcgttgccaaaatggatca-3′) and (5′-aaaaaccaacctcaagcatgtgg-3′) [48]. PCR amplification and detection were performed with the Applied Biosystems StepOnePlus Real-Time detector, using 2× SYBR GREEN Master Mix (Roche Diagnostic, Switzerland) as reagent, following the manufacturer's instructions. The reaction profile was denaturation-activation cycle (95 °C for 10 min) followed by 40 cycles of denaturation-annealing-extension (95 °C for 15 s, 60 °C for 60 s), and finally the melting curve analysis performed at 95 °C for 15 s, 60 °C for 60 s, and 95 °C for 15 s. mRNA levels were calculated using the StepOne™ software v2.3, following the $2^{-\Delta\Delta CT}$ method of Applied Biosystems [47]. The results were normalized for the expression levels of the housekeeping human *GAPDH* genes (5′-aggtcggtgtgaacggatttg-3′) and (5′-tgtagaccatgtagttgaggtca-3′), which were quantified simultaneously with the target gene [49].

2.5. Western blotting techniques

Soluble extracts from CCF-STTG1-cultured cells were processed for western blot. Cells were washed in 0.1 M phosphate-buffered saline (PBS) before collection in the sample buffer Laemmli (Sigma-Aldrich, Darmstadt, Germany). Then, homogenates were boiled at 95 °C for 10 min, followed by 12 % SDS-PAGE electrophoresis, and they were then electrotransferred to nitrocellulose membranes for 1 h at 4 °C. Membranes were blocked with 5 % non-fat milk in 0.1 M Tris-buffered saline (pH 7.4) for 1 h and incubated overnight in 0.5 % blocking solution containing primary antibodies. Monoclonal anti-PrP 6H4 (Prionics, Zurich, Switzerland) was used to determine PrP^C levels and monoclonal anti-α-actin (Merck Millipore) was used for standardization. After incubation with peroxidase-tagged secondary antibodies (1:5000 diluted), membranes were revealed with the ECL-plus chemiluminescence western blot kit (Amersham-GE Healthcare, UK).

For western blot quantification, developed films were scanned at 2400 × 2400 dpi (i800 MICROTEK high quality film scanner), and the densitometric analysis was performed using Fiji™ software (National Institutes of Health, USA).

2.6. miR-519a-3p target validation with dual-luciferase reporter assay

To determine targeting of miR-519a-3p to *PRNP* 3′UTR miRNA sequence, 4.5×10^4 HEK293 was seeded 24 h before transfection into 24-well plates. Cells were cotransfected with human *PRNP* 3′UTR miRNA Target Clone (pEZX-3′UTR-PRNP vector from Genecopoeia) at a final concentration of 1.25 ng/μl and 15 pmol of hsa-miR-519a-3p miRCURY LNA miRNA Mimic or its related Negative Control miRCURY LNA miRNA Mimic (Qiagen). Cell lysates were prepared 24 h later in passive lysis buffer following the manufacturer's instructions, and luciferase reported activity was measured with an Infinite M200 Pro Microplate Reader luminometer using the Dual-Luciferase assay system (Promega). Background luminosity was subtracted from un-transfected cells, and luciferase readings were normalized by dividing the reported gene firefly luciferase by the reference Renilla luciferase activity. Each construct was transfected in triplicate in three independent experiments.

2.7. Statistical processing

Data analysis was performed using Prism 8.0 (GraphPad Software, CA, USA). The differences between groups were obtained using Student *t*-test, and data were considered significant with $p < 0.05$, $p < 0.01$, $p < 0.001$, and $p < 0.0001$. All data are expressed as mean ± standard error of the mean (SEM). In addition, correlation analysis was made with the Pearson correlation coefficient. And receiver operating characteristic (ROC) curves were calculated for validation of potential clinical efficacy of miR-519a-3p in AD.

3. Results

3.1. miR-519a-3p overlaps PRNP 3′UTR in vitro and promotes changes in PrP^C

After identifying miR-519a-3p as a candidate to induce down-regulation in PrP^C during AD, we explored its functional activity in PrP^C

expression. To do this, we performed two parallel *in vitro* experiments using mimic technology. First, we analyzed the target of miR-519a-3p to *PRNP* 3′UTR using the pEZX-MT06-3′UTR-*PRNP* vector for Firefly luciferase expression under 3′UTR-*PRNP* control and Renilla luciferase for standardization. Two independent experiments were performed in three biological replicates (cells of three different passage numbers). 24 h after HEK293 co-transfection with miR-519a-3p mimic or its corresponding negative control and 3′UTR-*PRNP* construction, a dual-luciferase assay was performed using three technical replicates. Results showed a significant decrease of 21.12 % ± 1.40 in Firefly bioluminescence when miR-519a-3p mimic was expressed, confirming the predicted 3′UTR-*PRNP* site as a target for miRNA (Fig. 1A).

It is reported that miR-519a-3p only works on higher primate genomes, so the second approach was developed on *CCF-STTG1* cell line, a human astrocytoma line which presents high expression of PrP^C. Human cell line was transfected with miR-519a-3p mimic and with the negative control in parallel to measure later levels of both PrP^C protein and mRNA *PRNP*. Then, both RNA and protein were extracted at 12, 24, and 48 h after mimic transfection. Firstly, our results showed a progressive and significant increase in expression of miR-519a-3p by RT-qPCR (Supplementary Fig. 2). However, only the higher levels of miR-519a-3p, found at 48 h on three independent experiments with three technical replicates each (Fig. 1B), were associated with a significant decrease in PrP^C (45.79 % ± 5.23) with western blot analysis (Fig. 1C). mRNA *PRNP* levels analyzed with RT-qPCR remained unchanged (Fig. 1D), suggesting translational repression at this time point. Undepleted levels of both PrP^C protein and mRNA *PRNP* at 12 and 24 h after mimic transfection are shown in Supplementary Fig. 2.

3.2. Significant changes in miR-519a-3p levels at subclinical stages of AD

First, we aimed to determine miR-519a-3p levels in an early affected brain area in a small sample collection (Supplementary Table 1). Then, we performed a RT-qPCR and data were classified into 3 groups according to the Braak NFT stage of the patients. After comparison with nND, qPCR quantification of miR-519a-3p showed an increase in all three groups with a tendency to decrease with the progression of the disease: AD(I/II) (4.940 ± 0.829; $^{**}p = 0.0046$), AD(III/IV) (3.672 ± 0.890; $p = 0.0571$), and AD(V/VI) (1.844 ± 0.232; $^{*}p = 0.0405$) (Supplementary Fig. 3A). As *in silico* prediction of miRNAs made in this study pointed to additional three candidates (miR-409-3p, miR-410-3p, and miR-495-3p) [50], we extended the analysis to make a comparison with our preliminary results. After quantification, only miR-409-3p showed a slight increase in all three groups of analyzed AD samples, but with no statistical significance and without notable changes between groups (Supplementary Fig. 3B).

Looking at the significant increase in miR-519a-3p in hippocampal samples of the three AD groups, and, importantly, in non-symptomatic people AD(I/II), we aimed to determine miR-519a-3p levels in 'non-affected brain areas' of the same disease groups. Accordingly, we performed RT-qPCR in a larger collection of frontal cortex samples (Supplementary Table 2). Importantly, quantitative results again showed an increase in all three groups when compared to nND samples: AD(I/II) (1.883 ± 0.258; $^{**}p = 0.0012$), AD(III/IV) (2.484 ± 0.303; $^{****}p \leq 0.0001$) and AD(V/VI) (2.768 ± 0.554; $^{**}p = 0.0012$) (Fig. 2A). In addition, although there was a tendency to increase with the progression of the disease, we did not find statistically significant differences among

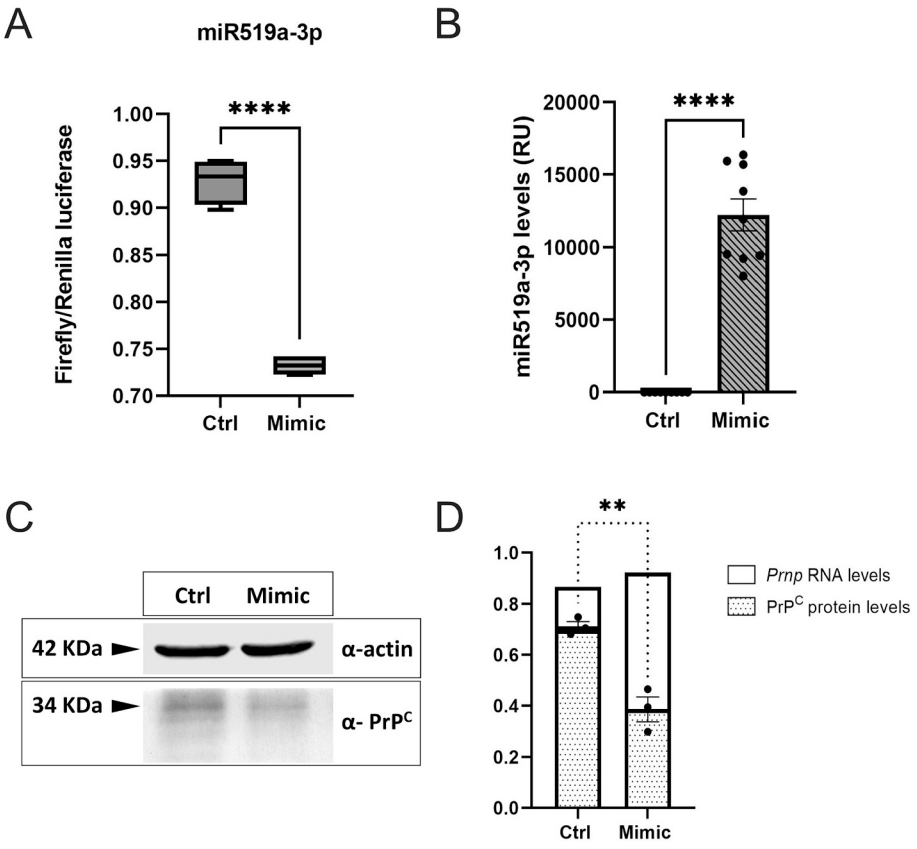

Fig. 1. Binding of miR-519a-3p mimic to the *PRNP* 3′UTR and decrease in PrP^C levels. Dual-luciferase reported assay showed the binding of miR-519a-3p to the *PRNP* 3′UTR after co-transfection of HEK293 cells with mimic and pEZX-3′UTR-*PRNP* vector by reduction of Firefly luciferase activity. Two independent experiments were performed in three biological replicates (A). Human CCF-STTG1 cell line shows overexpression of miR-519a-3p 48 h after transfection (B) and it is associated with a decrease of around 45 % in PrP^C protein levels (C, D) while mRNA levels remain unchanged (D). PrP^C, *PRNP* mRNA and miR-519a-3p were analyzed with western blot and RT-qPCR, respectively from three independent experiments. Differences between groups were considered statistically significant at $^{****}p < 0.0001$ and $^{*}p < 0.05$ (Student's *t*-test). RU: Relative units.

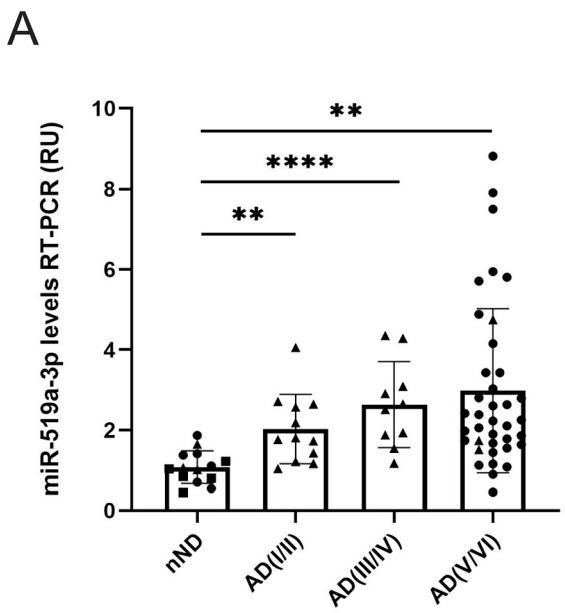

miR-519a-3p *vs.*	nND	AD
Age (years)	-0,097 *p*-value=0,741	0,211 *p*-value=0,105
Sex	0,195 *p*-value=0,505	0,073 *p*-value=0,582

Fig. 2. miR-519a-3p expression in frontal cortex samples with AD grouped according to NFT Braak staging (AD(I/II), AD(III/IV), and AD(V/VI)) and compared to nND samples. A. Histograms showing the RT-qPCR analysis of miR-519a-3p expression. The bars represent the mean of miRNA levels ± SEM between each group analyzed. Each dot represents the mean for the three technical replicates of each individual case (n = 14 nND, n = 12 AD(I/II), n = 11 AD(III/IV), and n = 38 AD(V/VI)), and the different shapes represent the biobank of origin: circle, BioBANC Clinic-IDIBAPS; triangle, HUB-ICO-IDIBELL Biobank; and square, NAVARRABIOMED Biobank. Differences between nND samples and the three AD groups were considered statistically significant at ****$p < 0.0001$ and **$p < 0.01$ (Student's *t*-test). RU: Relative units. B. Correlation data between miR-519a-3p levels and age or sex among individuals with AD and also, among nND samples. The table shows the Pearson's correlation coefficient and *p*-value for each case.

the 3 groups of affected people. The possible association between miR-519a-3p levels and age or gender was also investigated (Fig. 2B). After analysis, no correlation was found between the amount of miR-519a-3p and age in either the control group (nND) or among the AD affected population. A weak correlation could be assumed in the AD group (Pearson's coefficient = 0.211), although the *p*-value shows a non-statistical significance for the result ($p = 0.105$). Similarly, while only the nND group showed a weak correlation between miR-519a-3p levels and sex (Pearson's coefficient = 0.0195), it was not statistically significant ($p = 0.582$).

Finally, potential clinical efficacy of miR519a-3p in AD was tested with ROC curve analysis, from which we calculated area under the curve (AUC) with 95 % confidence intervals. Moreover, the cut-off was established based on sensitivity % and specificity % and quantification of positive predictive value (PPV) and negative predictive value (NPV) were carried out (Supplementary Fig. 4). Importantly, miR519a-3p showed a very good diagnostic potential already in the asymptomatic AD stages, based on the guide for assessing the utility of a biomarker based on its AUC: 0.9–1.0 = excellent; 0.8–0.9 = good; 0.7–0.8 = fair; 0.6–0.7 = poor; 0.5–0.6 = fail.

Specific pattern of miR-519a-3p expression in AD when compared with other NDD.

To further explore specific dysregulation of miR-519a-3p in AD, we analyzed the miRNA levels in additional samples from other NDDs that occur with accumulation of fibrillar proteins as in AD and in some cases with dementia as well, first examining several advanced non-AD tauopathies including a few representations of CBD, GGT, and PiD, and then, in various synucleopathies including PD and some cases of PDD classified into two groups according to staging of brain pathology related to sporadic PD. These groups are represented as PD(3–4) and PD(5–6), respectively (Supplementary Table 2).

Quantification of miR-519a-3p levels in advanced non-AD tauopathies compared to nND resulted in a non-significant increase of 1.282 ± 0.1999; $p = 0.1419$ (Fig. 3A). Similarly, we found no significant differences in either of the two groups of PD analyzed, despite the fact that

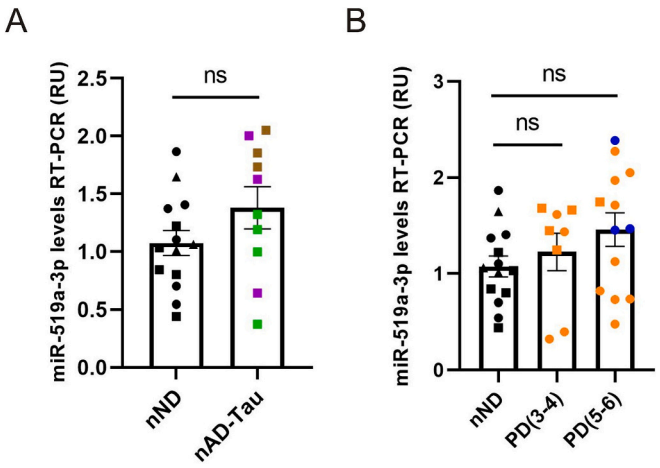

Fig. 3. miR-519a-3p expression in non-AD tauopathies (nAD-Tau) (A) and Parkinson's disease classified in PD(3–4) and PD(5–6) (B) compared to nND samples. Bars represent the mean of miRNA levels ± SEM between groups analyzed. Each dot represents the mean for the three technical replicates of each individual case while the different shapes corresponds to the Biobank of origin: circle, BioBANC Clinic-IDIBAPS; triangle, HUB-ICO-IDIBELL Biobank; and square, NAVARRABIOMED Biobank. In addition, the color code represents the neuropathological diagnoses of the samples: nND, black; PD, orange; PDD, blue; CBD, brown; GGT, violet; PiD, green. Differences between nND samples (n = 14) with nAD-Tau (n = 10), as with PD(3–4) (n = 8) and PD(5–6) (n = 13), were not considered statistically significant (Student's *t*-test). RU: relative units.

some of them presented dementia (Fig. 3B). The fold change of PD(3–4) compared to nND was 1.141 ± 0.2050; $p = 0.4673$ while the fold change of PD(5–6) compared to nND was 1.37 ± 0.2030; $p = 0.0705$.

Finally, we compared the AD cases distributed in groups AD(III/IV) and AD(V/VI) with the other NDD groups, non-AD tauopathies, PD (3–4), and PD(5–6). As observed in Fig. 4, the two AD groups showed

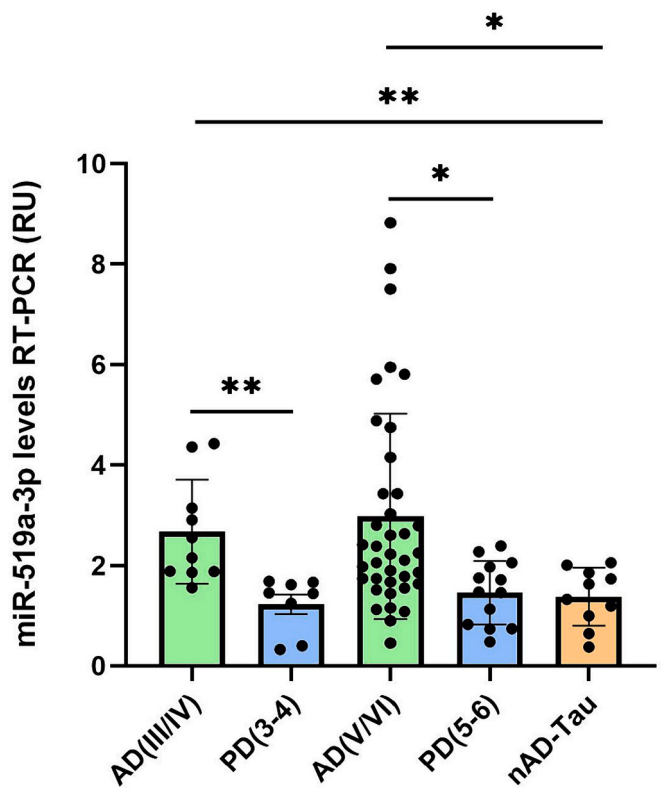

Fig. 4. miR-519a-3p expression in AD samples distributed in AD(III/IV) and AD (V/VI) groups and compared to nAD-Tau, PD(3–4), and PD(5–6) groups respectively. Bars represent the mean of miRNA levels ± SEM between each group analyzed. Each dot represents the mean for the three technical replicates of each individual case (n = 14 nND, n = 11 AD(III/IV), n = 8 PD(3–4), n = 38 AD(V/VI), n = 13 PD(5–6), and n = 10 nAD-Tau). Differences between AD, PD, and nAD-Tau samples were considered statistically significant at $^{**}p < 0.01$ and $^{*}p < 0.05$ (Student's *t*-test). RU: relative units.

much higher and significant values of miR-519a-3p than the other NDD groups analyzed. Specifically, the fold increase in the AD(III/IV) group was 2.176 ± 0.4074; $p = 0.0027$ when compared to PD(3–4) and 1.936 ± 0.3749; $p = 0.0029$ when compared to non-AD tauopathies. In addition, the increase in the AD(V/VI) group was 2.041 ± 0.5795; $p = 0.0117$ when compared to PD(5–6), and 2.158 ± 0.6578; $p = 0.0192$ when compared to non-AD tauopathies. Therefore, in all cases the results are alike when comparing AD with the nND controls.

Taken together, these results suggest that elevated levels of miR-519a-3p represent a new and specific early AD indicator.

4. Discussion

In the present study, we investigated two main issues concerning the role of miR-519a-3p in AD. On the one hand, there is its possible involvement in reducing PrP^C expression levels in the evolution of the disease [42,51]. In fact, the role of PrP^C in AD and other NDDs is still a matter of debate, as some argue for its neuroprotective function while others point to it as an enhancer of the neurotoxicity associated with NDD (discussed in [32]). This is why it is important to identify the factors that modulate its expression levels, causing the protein to show increased levels in the brain parenchyma of patients in asymptomatic stages of AD and decreasing levels as the disease progresses.

The second issue to investigate is the potential use of this miRNA as a biomarker for the detection of AD in its asymptomatic stages. Up-regulation of some family members of miR-519 has been widely reported in various tissues from AD patients, *e.g.*, FC [44], CSF [23], and in blood (plasma or serum) [22,24,25]. In fact, the latter points to miR-519d-3p as a bridge regulator between MCI and AD. However, scant attention has been paid to analyzing up-regulation of any member of the miR-519 family in asymptomatic people who may have initiated the disease silently (with Braak stage I–II correlation) [9].

In our study, *in silico* prediction of potential miRNAs with *PRNP* 3′UTR as target pointed to miR-519a-3p [44], among others, as a candidate that is up-regulated in AD. Importantly, binding of other miR-519 family members (b-3p and d-3p) to *PRNP* 3′UTR and the consequent mRNA degradation has already been demonstrated *in vitro* [43]. It is further assumed that mature miRNAs belonging to the same family share the same target genes according to conserved regions in their sequences [52]. Specifically, miR-519a-3p and miR-519b-3p belong to the same subfamily, so they share exactly the same seed sites, while miR-519d-3p is part of the AGUGC family like both of them [53]. Thus, our results using mimic technology corroborate the control of PrP^C expression by this additional miR-519 family member, first, determining miR-519a-3p target validation with dual-luciferase reporter assay, and secondly, downregulating PrP^C protein levels after miR-519a-3p mimic overexpression. However, in contrast to previous data, our experiment elicited translational repression and not mRNA degradation, since *PRNP* mRNA levels did not change. Perhaps the time point at which we measured PrP^C protein and *PRNP* mRNA levels was decisive in this regard, because we analyzed the samples up to 48 h after mimic transfection while they did so at 72 h [43].

Amyloid deposition in the hippocampus, one of the earliest hallmarks of AD, is the main cause of neural degeneration and associated dementia [54]. Therefore, we analyzed four previously reported up-regulated miRNAs in the disease, miR-519a-3p [44], miR-409-3p, miR-410-3p, and miR-495-3p [50] in hippocampal brain tissue from Braak I to VI AD and non-AD affected people. RT-qPCR results showed a significant up-regulation of miR-519a-3p in AD samples but no significant changes in the other selected miRNAs. Although our results did not correlate with [50], it is important to note that the aforementioned study, as well as Lau et al. [44], were carried out on frontal cortex samples. Even so, the quantification of miR-519a-3p correlated with results from Lau et al. [44], which is why we extended the study to one brain area affected later in the disease, as is the frontal cortex. After analyzing the miR-519a-3p levels in the 61 frontal cortex samples of AD, we corroborated the significant up-regulation in Braak III-IV compared to non-AD samples. This is why these results support the possible use of miR-519a-3p in the detection of patients presenting MCI as suggested in Tao et al. [24]. However, our results also show that this miRNA is significantly up-regulated in apparently asymptomatic Braak I-II samples, as identified at the time of the post-mortem neuropathological examination. In fact, elevated levels of miR-519a-3p have previously been reported in prefrontal cortex from late-onset AD Braak I patients [44], although the focus of the aforementioned study was on the identification of miRNAs directly implicated in pathogenesis of the disease, and no attention was paid to possible biomarkers. This finding, together with its already reported detection in blood of AD patients [24,25], makes miR-519a-3p a putative diagnostic tool for the disease.

It would have been interesting to be able to establish correlations between miR-519a-3p levels and clinical data of the subjects analyzed (*e.g.* disease duration, cognitive test scores…). However, these data do not exist for the sample group Braak I–II, which we can consider the most important in this study. Even so, the correlation between serum miR519 levels and MMSE score has already been ruled out in patients with probable AD by Jia and Liu [22].

As further information, some of the samples included in this study had previously been analyzed for *PRNP* mRNA levels. In this sense, it can be observed how protein levels in hippocampal samples suffer a greater drop than mRNA levels with disease progression [51]. Similarly, analysis of frontal cortex samples points to a trend towards mRNA reduction only in advanced stages of the disease (Supplementary Fig. 5). According to Pease et al. [43] and our *in vitro* studies, this would be consistent with a different time point between translational repression and mRNA

degradation promoted by miR-519a-3p.

There currently exist several blood-based biomarkers that correlate well with the classical diagnosis of the disease by means of CSF analysis or imaging tests. Specifically, these are MRI for the detection of brain atrophy and PET with radiotracers for the detection of Aβ or phospho-tau deposits [18,55–58]. However, these emerging biomarkers cannot detect pre-clinical disease since differential levels of them are detectable only when the degenerative process starts showing signs of dementia [59].

Several studies show the potential of miRNAs as diagnostic tools due to their stability and abundance in circulatory fluids (reviewed in [20]. The 'golden' indicator of RNA degradation is the 'RNA integrity number' (RIN) that cannot be applied to miRNAs which are extremely stable against nucleases [60]. Our results have shown the non-association between RIN and miR-519a-3p level which only depends on AD evolution (Supplementary Fig. 6). But more importantly, miRNAs show a regular pattern of expression among various body fluids including blood-based fluids, which facilitates their extraction with non-invasive methods for diagnostic use [19]. In addition, miRNAs can cross the blood brain barrier (BBB) [61], and correlation between miRNA expression levels in plasma and brain parenchyma has been reported [21].

Although other neurodegenerative diseases such as PD and tauopathies may present with dementia like AD, most of them show diagnoses well-differentiated from AD. This is not always the case, as hippocampal atrophy on magnetic resonance imaging (MRI) is an early characteristic of AD that may also occur in other dementias, such as FTLD [62]. Also, comorbid proteinopathies are frequent in these pathologies [63]. Even so, if we consider the hypothetically healthy population as a target for screening miR-519a-3p levels, it is important to ensure that other NDDs that, like AD, course with self-aggregation of proteins with spreading properties do not also converge in the up-regulation of this miRNA. In this regard, miRNA dysregulation has previously been reported in both tauopathies and synucleopathies [64,65]. We have therefore considered it important to compare the miR-519a-3p levels found in some other non-AD tauopathies (CBD, GGT and PiD) and in some cases of synucleopathies (PD and PDD). To date, the presence of miR-519a-3p has never been analyzed in tauopathies, while in the case of synucleopathies, only analysis on IPSC-derived neurons from PD patients has been made, with miR-519 reduction reported [66]. It should be added that in addition to the PD and PDD cases shown in our study, 19 additional cases also presenting Alzheimer-related pathology (ARP) were analyzed. All of them were classified according to Braak NFT stages and Aβ deposition. However, in none of the cases were significant differences found between miR-519a-3p levels in the aforementioned samples when compared to nND cases (data not shown). The did show significant differences when compared with the cases of AD. These results, then, ruled out an association between miR-519a-3p and Aβ plaques. Our results point to increased miR-519a-3p levels as a novel specific sign of AD (independently of NFT lesions and Aβ deposition stage) that serves as a promising tool in the attempt to determine whether a person is in the asymptomatic stage of the disease. The next step is to start checking blood-derived samples of different cohorts that have been followed up longitudinally to implement the clinical use of miR-519a-3p in the diagnosis of AD. Importantly, correlation analyses between miR-519a-3p levels and clinical data of the different subjects may be included in the study.

5. Conclusions

The present study points to miR-519a-3p as one of the elements responsible for the decrease in PrP^C in AD progression. The early expression of this miRNA in the disease is of great interest to be included in a disease-specific asymptomatic AD signature with a great potential to become a blood-based biomarker that merits further study.

Funding statement

This research was supported by PRPCDEVTAU (PID2021-123714OB-I00), ALTERNED (PLEC2022-009401) and PDC2022-133268-I00 funded by MCIN/AEI/10.13039/501100011033 and by "ERDF A way of making Europe", the CERCA Programme, Ciberned Institute Carlos III (NESDG114 and NED21PI02DR) and the Commission for Universities and Research of the Department of Innovation, Universities, and Enterprise of the Generalitat de Catalunya (SGR2021-00453). The project leading to these results received funding from the María de Maeztu Unit of Excellence (Institute of Neurosciences, University of Barcelona) and Severo Ochoa Unit of Excellence (Institute of Bioengineering of Catalonia).

Ethics approval statement

All postmortem human brains, from Clinic-IDIBAPS, HUB-ICO-IDIBELL, and NAVARRABIOMED Biobanks, were obtained following the guidelines of Spanish legislation on this matter (Real Decreto 1716/2011), and the approval of the local ethics committees (Approval numbers/ID: 2016/13456, PR198/17 and 2020/CEIC/350).

CRediT authorship contribution statement

Dayaneth Jácome: Methodology, Investigation, Formal analysis. **Tiziana Cotrufo:** Writing – review & editing, Investigation. **Pol Andrés-Benito:** Writing – review & editing, Investigation. **Laia Lidón:** Writing – review & editing, Investigation. **Eulàlia Martí:** Writing – review & editing, Software. **Isidre Ferrer:** Writing – review & editing, Data curation. **José Antonio del Río:** Writing – review & editing, Funding acquisition. **Rosalina Gavín:** Writing – review & editing, Writing – original draft, Investigation, Formal analysis, Conceptualization.

Declaration of competing interest

The authors declare no conflicts of interest.

Data availability

Data will be made available on request.

Acknowledgments

The authors thank Tom Yohannan for editorial advice and Miriam Segura-Feliu and Juan José López Jiménez for technical help. We also thank the Core facilities of IBEC for technical help.

Appendix A. Supplementary data

Supplementary data to this article can be found online at https://doi.org/10.1016/j.bbadis.2024.167187.

References

[1] J. Avila, Tau aggregation into fibrillar polymers: taupathies, FEBS Lett. 476 (1–2) (2000) 89–92.
[2] H. Braak, E. Braak, Neuropathological stageing of Alzheimer-related changes, Acta Neuropathol. 82 (4) (1991) 239–259.
[3] H. Braak, E. Braak, et al., Age, neurofibrillary changes, a beta-amyloid and the onset of Alzheimer's disease, Neurosci. Lett. 210 (2) (1996) 87–90.
[4] K. Iqbal, E. Braak, et al., A silver impregnation method for labeling both Alzheimer paired helical filaments and their polypeptides separated by sodium dodecyl sulfate-polyacrylamide gel electrophoresis, Neurobiol. Aging 12 (4) (1991) 357–361.
[5] A. Serrano-Pozo, M.P. Frosch, et al., Neuropathological alterations in Alzheimer disease, Cold Spring Harb. Perspect. Med. 1 (1) (2011) a006189.
[6] H. Braak, E. Braak, Evolution of the neuropathology of Alzheimer's disease, Acta Neurol. Scand. Suppl. 165 (1996) 3–12.

[7] V.J. Lowe, E.S. Lundt, et al., Neuroimaging correlates with neuropathologic schemes in neurodegenerative disease, Alzheimers Dement. 15 (7) (2019) 927–939.
[8] T. Tapiola, I. Alafuzoff, et al., Cerebrospinal fluid {beta}-amyloid 42 and tau proteins as biomarkers of Alzheimer-type pathologic changes in the brain, Arch. Neurol. 66 (3) (2009) 382–389.
[9] C.M. Wischik, C.R. Harrington, et al., Tau-aggregation inhibitor therapy for Alzheimer's disease, Biochem. Pharmacol. 88 (4) (2014) 529–539.
[10] B. Dubois, S. Bombois, et al., Toward a preventive management Alzheimer's disease, Bull. Acad. Natl. Med. 204 (6) (2020) 583–588.
[11] H. Hampel, S.E. O'Bryant, et al., A precision medicine initiative for Alzheimer's disease: the road ahead to biomarker-guided integrative disease modeling, Climacteric 20 (2) (2017) 107–118.
[12] H. Hampel, N. Toschi, et al., Alzheimer's disease biomarker-guided diagnostic workflow using the added value of six combined cerebrospinal fluid candidates: Abeta1-42, total-tau, phosphorylated-tau, NFL, neurogranin, and YKL-40, Alzheimers Dement. 14 (4) (2018) 492–501.
[13] H. Lee, D. Ugay, et al., Alzheimer's disease diagnosis using misfolding proteins in blood, Dement. Neurocogn. Disord. 19 (1) (2020) 1–18.
[14] H. Zetterberg, S.C. Burnham, Blood-based molecular biomarkers for Alzheimer's disease, Mol. Brain 12 (1) (2019) 26.
[15] I. de Rojas, J. Romero, et al., Correlations between plasma and PET beta-amyloid levels in individuals with subjective cognitive decline: the Fundacio ACE Healthy Brain Initiative (FACEHBI), Alzheimers Res. Ther. 10 (1) (2018) 119.
[16] S.L. Risacher, N. Fandos, et al., Plasma amyloid beta levels are associated with cerebral amyloid and tau deposition, Alzheimers Dement. (Amst.) 11 (2019) 510–519.
[17] A. Leuzy, N. Mattsson-Carlgren, et al., Blood-based biomarkers for Alzheimer's disease, EMBO Mol. Med. 14 (1) (2022) e14408.
[18] C.E. Teunissen, I.M.W. Verberk, et al., Blood-based biomarkers for Alzheimer's disease: towards clinical implementation, Lancet Neurol. 21 (1) (2022) 66–77.
[19] C. Cui, Q. Cui, The relationship of human tissue microRNAs with those from body fluids, Sci. Rep. 10 (1) (2020) 5644.
[20] J. Hanna, G.S. Hossain, et al., The potential for microRNA therapeutics and clinical research, Front. Genet. 10 (2019) 478.
[21] M.Z. Kos, S. Puppala, et al., Blood-based miRNA biomarkers as correlates of brain-based miRNA expression, Front. Mol. Neurosci. 15 (2022) 817290.
[22] L.H. Jia, Y.N. Liu, Downregulated serum miR-223 servers as biomarker in Alzheimer's disease, Cell Biochem. Funct. 34 (4) (2016) 233–237.
[23] T.A. Lusardi, J.I. Phillips, et al., MicroRNAs in human cerebrospinal fluid as biomarkers for Alzheimer's disease, J. Alzheimers Dis. 55 (3) (2017) 1223–1233.
[24] Y. Tao, Y. Han, et al., The predicted key molecules, functions, and pathways that bridge mild cognitive impairment (MCI) and Alzheimer's disease (AD), Front. Neurol. 11 (2020) 233.
[25] Y. Zhao, Y. Zhang, et al., The potential markers of circulating microRNAs and long non-coding RNAs in Alzheimer's disease, Aging Dis. 10 (6) (2019) 1293–1301.
[26] S.B. Prusiner, Novel proteinaceous infectious particles cause scrapie, Science 216 (4542) (1982) 136–144.
[27] H.H. Griffiths, I.J. Whitehouse, et al., Regulation of amyloid-beta production by the prion protein, Prion 6 (3) (2012) 217–222.
[28] H. Nieznanska, S. Boyko, et al., Neurotoxicity of oligomers of phosphorylated Tau protein carrying tauopathy-associated mutation is inhibited by prion protein, Biochim. Biophys. Acta Mol. basis Dis. 1867 (11) (2021) 166209.
[29] E.T. Parkin, N.T. Watt, et al., Cellular prion protein regulates beta-secretase cleavage of the Alzheimer's amyloid precursor protein, Proc. Natl. Acad. Sci. U. S. A. 104 (26) (2007) 11062–11067.
[30] J. Lauren, D.A. Gimbel, et al., Cellular prion protein mediates impairment of synaptic plasticity by amyloid-beta oligomers, Nature 457 (7233) (2009) 1128–1132.
[31] L. Westergard, H.M. Christensen, et al., The cellular prion protein (PrP(C)): its physiological function and role in disease, Biochim. Biophys. Acta 1772 (6) (2007) 629–644.
[32] R. Gavin, L. Lidon, et al., The quest for cellular prion protein functions in the aged and neurodegenerating brain, Cells 9 (3) (2020).
[33] M.J. Ford, L.J. Burton, et al., Selective expression of prion protein in peripheral tissues of the adult mouse, Neuroscience 113 (1) (2002) 177–192.
[34] F.J. Moleres, J.L. Velayos, Expression of PrP(C) in the rat brain and characterization of a subset of cortical neurons, Brain Res. 1056 (1) (2005) 10–21.
[35] M. Moser, R.J. Colello, et al., Developmental expression of the prion protein gene in glial cells, Neuron 14 (3) (1995) 509–517.
[36] O. Nicolas, R. Gavin, et al., New insights into cellular prion protein (PrPc) functions: the "ying and yang" of a relevant protein, Brain Res. Rev. 61 (2) (2009) 170–184.
[37] G. Miele, A.R. Alejo Blanco, et al., Embryonic activation and developmental expression of the murine prion protein gene, Gene Expr. 11 (1) (2003) 1–12.
[38] A. Miranda, P. Ramos-Ibeas, et al., The role of prion protein in stem cell regulation, Reproduction 146 (3) (2013) R91–R99.
[39] I.J. Whitehouse, C. Jackson, et al., Prion protein is reduced in aging and in sporadic but not in familial Alzheimer's disease, J. Alzheimers Dis. 22 (3) (2010) 1023–1031.
[40] A. McNeill, A molecular analysis of prion protein expression in Alzheimer's disease, McGill J. Med. 8 (2004) 7–14.
[41] P. Rezaie, C.C. Pontikis, et al., Expression of cellular prion protein in the frontal and occipital lobe in Alzheimer's disease, diffuse Lewy body disease, and in normal brain: an immunohistochemical study, J. Histochem. Cytochem. 53 (8) (2005) 929–940.
[42] C. Vergara, L. Ordonez-Gutierrez, et al., Role of PrP(C) expression in tau protein levels and phosphorylation in Alzheimer's disease evolution, Mol. Neurobiol. 51 (3) (2015) 1206–1220.
[43] D. Pease, C. Scheckel, et al., Genome-wide identification of microRNAs regulating the human prion protein, Brain Pathol. 29 (2) (2019) 232–244.
[44] P. Lau, K. Bossers, et al., Alteration of the microRNA network during the progression of Alzheimer's disease, EMBO Mol. Med. 5 (10) (2013) 1613–1634.
[45] H. Braak, E. Braak, et al., Evolution of Alzheimer's disease related cortical lesions, J. Neural Transm. Suppl. 54 (1998) 97–106.
[46] H. Braak, K. Del Tredici, et al., Staging of brain pathology related to sporadic Parkinson's disease, Neurobiol. Aging 24 (2) (2003) 197–211.
[47] K.J. Livak, T.D. Schmittgen, Analysis of relative gene expression data using real-time quantitative PCR and the $2^{-\Delta\Delta C(T)}$ method, Methods 25 (4) (2001) 402–408.
[48] A. Bribian, X. Fontana, et al., Role of the cellular prion protein in oligodendrocyte precursor cell proliferation and differentiation in the developing and adult mouse CNS, PloS One 7 (4) (2012) e33872.
[49] P. Carulla, A. Bribian, et al., Neuroprotective role of PrPC against kainate-induced epileptic seizures and cell death depends on the modulation of JNK3 activation by GluR6/7-PSD-95 binding, Mol. Biol. Cell 22 (17) (2011) 3041–3054.
[50] I. Santa-Maria, M.E. Alaniz, et al., Dysregulation of microRNA-219 promotes neurodegeneration through post-transcriptional regulation of tau, J. Clin. Invest. 125 (2) (2015) 681–686.
[51] L. Lidon, L. Llao-Hierro, et al., Tau exon 10 inclusion by PrP(C) through downregulating GSK3beta activity, Int. J. Mol. Sci. 22 (10) (2021).
[52] Y. Cai, X. Yu, et al., A brief review on the mechanisms of miRNA regulation, Genomics Proteomics Bioinformatics 7 (4) (2009) 147–154.
[53] Z. Wang, miRNA interference technologies, in: MicroRNA Interference Technologies, Springer Berlin Heidelberg, Berlin, Heidelberg, 2009, pp. 59–73.
[54] D.C. Woodworth, N. Sheikh-Bahaei, et al., Dementia is associated with medial temporal atrophy even after accounting for neuropathologies, Brain Commun. 4 (2) (2022) fcac052.
[55] N.C. Cullen, A. Leuzy, et al., Plasma biomarkers of Alzheimer's disease improve prediction of cognitive decline in cognitively unimpaired elderly populations, Nat. Commun. 12 (1) (2021) 3555.
[56] A. Leuzy, N.C. Cullen, et al., Current advances in plasma and cerebrospinal fluid biomarkers in Alzheimer's disease, Curr. Opin. Neurol. 34 (2) (2021) 266–274.
[57] R. Ossenkoppele, J. Reimand, et al., Tau PET correlates with different Alzheimer's disease-related features compared to CSF and plasma p-tau biomarkers, EMBO Mol. Med. 13 (8) (2021) e14398.
[58] H. Zetterberg, B.B. Bendlin, Biomarkers for Alzheimer's disease-preparing for a new era of disease-modifying therapies, Mol. Psychiatry 26 (1) (2021) 296–308.
[59] I. Ferrer, Hypothesis review: Alzheimer's overture guidelines, Brain Pathol. 33 (1) (2023) e13122.
[60] M. Jung, A. Schaefer, et al., Robust microRNA stability in degraded RNA preparations from human tissue and cell samples, Clin. Chem. 56 (6) (2010) 998–1006.
[61] O. Beylerli, I. Gareev, et al., The role of microRNA in the pathogenesis of glial brain tumors, Noncoding RNA Res. 7 (2) (2022) 71–76.
[62] L.A. van de Pol, A. Hensel, et al., Hippocampal atrophy on MRI in frontotemporal lobar degeneration and Alzheimer's disease, J. Neurol. Neurosurg. Psychiatry 77 (4) (2006) 439–442.
[63] G.G. Kovacs, Are comorbidities compatible with a molecular pathological classification of neurodegenerative diseases? Curr. Opin. Neurol. 32 (2) (2019) 279–291.
[64] Y.H. Nies, N.H. Mohamad Najib, et al., MicroRNA dysregulation in Parkinson's disease: a narrative review, Front. Neurosci. 15 (2021) 660379.
[65] D. Pratico, The functional role of microRNAs in the pathogenesis of tauopathy, Cells 9 (10) (2020).
[66] E. Tolosa, T. Botta-Orfila, et al., MicroRNA alterations in iPSC-derived dopaminergic neurons from Parkinson disease patients, Neurobiol. Aging 69 (2018) 283–291.